

## Phenomena Due to Strain Coupling in Phase Transitions

Simon Marais,<sup>(1)</sup> Volker Heine,<sup>(1)</sup> Chris Nex,<sup>(1)</sup> and Ekhard Salje<sup>(2)</sup>

<sup>(1)</sup>*Cavendish Laboratory, University of Cambridge, Madingley Road, Cambridge, CB3 0HE, England*

<sup>(2)</sup>*Department of Earth Sciences, University of Cambridge, Downing Street, Cambridge, CB2 3EQ, England*

(Received 26 November 1990)

A theoretical model of an order-disorder phase transition in a crystal has been developed with strain-induced coupling between Ising spins. Strain coupling leads to long-ranged renormalized interactions between the spins which result in ferroelastic-antiferroelastic phase transitions. Computer simulations show textured microstructures evolving for some cases, similar to tweed textures. In other cases the long correlation length of strain suppresses nucleation, and the rate of (dis)ordering follows mean-field theory, very different from "nucleation and growth."

PACS numbers: 64.60.Qb, 81.30.Hd

Strain is now recognized as playing a very important role in a wide variety of order-disorder structural phase transitions in crystals. In some cases the strain energy accounts for up to 50% of the total energy.<sup>1,2</sup> Its characteristic feature is the long-range nature of the elastic forces. If the microscopic process that creates the strain (e.g., cation ordering in calcite or silicates) is modeled by an Ising "spin" that is coupled locally to the lattice atoms, the elastic forces within the material lead to a renormalized coupling  $J_{ij}$  between the Ising spins which reaches far into the lattice. We believe that the long-range nature of the coupling is responsible for such experimental observations in order-disorder phase transitions as the occurrence of textured microstructures<sup>2</sup> and the apparent mean-field behavior in some cases over large temperature intervals.<sup>3</sup>

In order to help understand such phenomena,<sup>4</sup> we have developed an Ising model in which the effective interaction between spins is purely indirect, via local coupling of the spins to an elastic lattice. After all, the size of atoms is the most fundamental factor determining crystal structures, and in our model driving the ordering process. It represents a new paradigm showing new phenomena compared with nearest-neighbor Ising models which have been the traditional paradigm in the study of (dis)order structural phase transitions. The model has been studied analytically and by computer simulation for spin-lattice couplings of various symmetries. The main results are as follows. (a) The indirect coupling between spins via local strain effects can lead to both ferroelastic and antiferroelastic order. (b) In most cases the  $16 \times 16 \times 16$  simulation model (dis)orders *uniformly*, not by nucleation and growth mechanisms. This contrasts with a traditional nearest-neighbor Ising model. (c) In such cases the (dis)ordering kinetics are described quite accurately by a mean-field theory (MFT). (d) In a few cases with couplings of particular symmetry related to that of the elastic lattice, one finds on quenching the sample that a dense texture of "stripe" or "tweed" form develops.

Our model is illustrated in Fig. 1. We consider a lattice of atoms ( $16 \times 16 \times 16$  in the simulation). In each unit cell  $i$  we have an Ising spin  $\sigma_i = \pm 1$  [Fig. 1(a)], taken to represent some internal ordering process which is not further specified, but which may be imagined to be like that shown in Fig. 1(b), for example. We assume a set of forces  $\mathbf{K}_{in}$  on the set of eight corner atoms  $n$  surrounding spin  $i$ , such as shown in Fig. 1(a), with the sign depending on the sign of  $\sigma_i$ . The atoms of the lattice are connected by harmonic springs between nearest and next-nearest neighbors of strength  $A^{(1)}$  and  $A^{(2)}$ . There is no direct coupling between the spins. However, spin  $i$  deforms the lattice around itself through the forces  $\mathbf{K}_{in}$ , and the deformation is transmitted through the elastic lattice via the springs to the atoms around spin  $j$ , which in turn is acted on via the couplings  $\mathbf{K}_{jm}$ . The result is

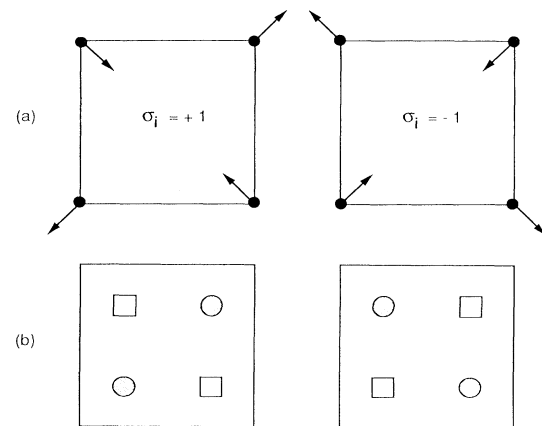


FIG. 1. Two-dimensional sketch of our three-dimensional model, showing one unit cube of the simple cubic lattice of atoms denoted by solid circles. (a) A set of forces  $\mathbf{K}_{in}$  on the corner atoms depending on whether  $\sigma_i = +1$  or  $-1$  with the symmetry of the macroscopic strain  $e_{xy}$ . (b) Possible ordering scheme of two types of atoms (open circles and squares) inside the unit cell giving rise to and having the symmetry of the forces in (a).

an effective or indirect coupling  $J_{ij}$  via the lattice. In the simulations there are  $15^3$  spins corresponding to the  $16^3$  atoms, and the atoms on the surface of the cluster are allowed to relax freely without the imposition of periodic boundary conditions or other forces or constraints.

For computational convenience the array of springs was mostly taken to have cubic symmetry, but some tests showed that this did not alter the phenomena significantly. A more serious shortcoming of the model is the use of an Ising spin in cases where the order parameter should be represented by a generalized  $n$ -state Potts model, e.g., the eight orientations of the  $\text{CN}^-$  ion along the (111) directions in cubic KCN. There are then  $n$  possible types of domain, but the domain walls between them will be governed by the same general considerations discussed below. The detailed structure of the texture will be different, but not the qualitative features controlling its presence and scale.

We may make our model mathematical by writing the Hamiltonian<sup>4</sup>

$$H = u^T A u - 2\sigma^T K u, \quad (1)$$

where  $u$  is the column vector of the displacements of all the atoms from their lattice sites,  $\sigma$  is the column vector of all the  $\sigma_i$ , and  $T$  denotes transpose. Also,  $A$  is the dynamical force matrix and  $K$  the matrix of spin-strain coupling. The Hamiltonian can be decoupled by considering

$$\bar{u} = u - A^{-1} K^T \sigma \quad (2)$$

as a set of displaced "oscillator" coordinates, in terms of which  $H$  becomes

$$H = \bar{u}^T A \bar{u} - \sigma^T J \sigma, \quad (3)$$

with

$$J = K A^{-1} K^T. \quad (4)$$

Here  $J_{ij}$  is the matrix of effective interactions. Its long-range nature can be appreciated from the elementary analysis of an expanded hole in a rubber ball.<sup>5</sup>

There are 24 linearly independent sets of forces  $K_{in}$  which can be formed using the  $x$ ,  $y$ , and  $z$  directions and eight corner atoms of the unit cell. Of course, more complicated structures and more distant forces allow an even larger number. Our 24 sets fall into three classes: class 1, six correspond to uniform translations and rotations of the cell; class 2, six result in the macroscopic strains  $e_{xx}$ ,  $e_{xy}$ , etc.; and class 3, twelve are orthogonal to the above. Of course, linear combinations of these are possible, e.g., an ordering process with tetragonal symmetry coupling to<sup>6,7</sup>  $3e_{zz} - (e_{xx} + e_{yy} + e_{zz})$  or even a combination of representations from both classes 2 and 3 as, e.g., in our modeling of the Cu-O planes in high- $T_c$  superconductors.

It can be shown that class 1 gives no effective coupling, as might be expected. The couplings of class 2 al-

ways result in ferroelastic ordering, i.e., an order parameter  $Q_q$  with wave vector  $q=0$ . On the other hand, the couplings of class 3 give various patterns of antiferroelastic ordering of the spins corresponding to order parameters  $Q_q$  with  $q$  at various points on the Brillouin-zone boundary.

While a consideration of a purely dilational coupling (ordering of large and small atoms in a simple metallic structure) is not new,<sup>8-10</sup> we believe ours is the first systematic study of the possible range of effects. More details will be given elsewhere.<sup>11</sup> For Al/Si ordering in complex silicates, not to mention perovskites and other materials, a wide range of symmetry types are indeed relevant to real materials of interest. Note that we use the expression "strain coupling" for class 3 as well as class 2, because there is little difference at the atomic level, and indeed class 3 appears to be the more common.<sup>12</sup>

We have investigated the nature of the  $J_{ij}$  and their variation with distance  $r_{ij}$ . This has been carried out numerically and analytically.<sup>4</sup> The  $J_{ij}$  of classes 2 and 3 have a strong short-range part that tends to vary somewhat erratically and even oscillate in sign. At intermediate distances they fall off as  $r_{ij}^{-4}$  and  $r_{ij}^{-5}$ , respectively, which we can count as long range in nature. In the case of class 2 there is also a constant term independent of distance (i.e., of infinite range), in magnitude inversely proportional to the size of the cluster so that its contribution to

$$J_{\text{tot}} = \sum_j J_{ij} \quad (5)$$

is a constant. Incidentally,  $J_{\text{tot}}$  can be calculated directly by energy-balance methods.<sup>4</sup>

The first test was to check that on cooling from a disordered state at high temperature  $T$  the model goes through a second-order phase transition at some  $T_c$ . Indeed, the order parameter  $Q(T)$  below  $T_c$  follows closely that of an Ising model treated in MFT, as might be expected from the long-range nature of the  $J_{ij}$ . Several sets of forces of different symmetries were tested. The Metropolis algorithm with Glauber dynamics<sup>13</sup> was used on the spins and the lattice atoms adjusted to their equilibrium positions after each Monte Carlo step. The observed value of  $T_c$  was somewhat ( $\sim 10\%$ ) below the theoretical Bragg-Williams value of  $T_c$  due to finite-size effects in our small computer sample and from some short-range correlation from the strong  $J_{ij}$  between near neighbors.

The model shows at least two features which contrast with those of the standard nearest-neighbor Ising model. In a few symmetry cases, on quenching from high  $T$  to below  $T_c$  the simulation system would get into a metastable state showing a rich texture of domains in the shape of short stripes running in two perpendicular directions, very reminiscent of the tweed texture observed in many materials including alloys and minerals.<sup>2</sup> In all

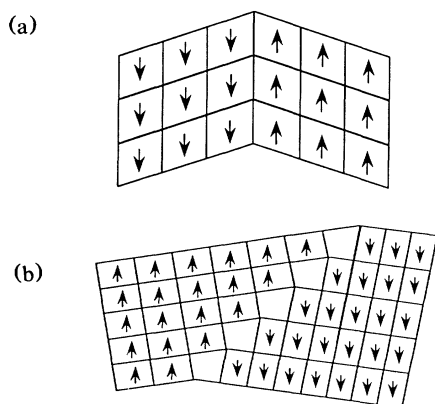


FIG. 2. (a) Zero-energy domain wall for  $XY$  strain coupling. (b) No such wall is possible for  $2Z^2 - X^2 - Y^2$  strain coupling.

cases the occurrence and scale of the texture could be accounted for by two principles. First, atomically coherent domain walls of strain  $e^{(1)}$  and  $e^{(2)}$  can only exist if the matrix  $(e^{(1)} - e^{(2)})_{ij}$  satisfies certain mathematical criteria.<sup>14</sup> Second, domain walls, if they exist, can be of two types, (a) and (b), shown in Figs. 2(a) and 2(b), respectively. Type (a) has zero domain-wall energy, giving domains only one or two cells wide in our simulations, as occurs for a strain coupling of  $e_{xy}$  symmetry [Fig. 2(a)]. With type (b) the wall energy is not zero because of the layer of distorted cells along the boundary as happens with  $e_{xx} - e_{yy}$  strain coupling [Fig. 2(b)]. Elastic relaxation gives walls a few cells wide, interactions between walls, and texture on a scale of ten cells, occasionally seen in our small simulation sample but prominent in a larger  $100 \times 100$  two-dimensional simulation.<sup>15</sup> Note that a coupling of type  $e_{xx} - e_{yy}$  is macroscopically equivalent to  $e_{xy}$  strain coupling rotated through  $45^\circ$ , but differs on the atomic scale with very different results. Antiferroelectric domain walls can also belong to types (a) and (b).

The other new feature concerns kinetics. Except in the cases where the above texture is observed, the system in a simulated quench orders rather uniformly. Because of the long-range nature of the interaction each spin "feels" others ordering throughout the system, as appears to be observed in most ferroelastics [e.g.,  $\text{Pb}_3(\text{PO}_4)_2$ ]. It is quite different from the ordering in a nearest-neighbor Ising system which proceeds by the traditional process of nucleation and growth of small clusters.<sup>16</sup> The difference is demonstrated in Fig. 3 which plots the distribution of a coarse-grained order parameter  $Q$  as the system orders ferroelastically. Initially  $Q$  is distributed around zero with statistical width of  $1/\sqrt{27}$  as expected from the  $3 \times 3 \times 3$  coarse graining (Fig. 3). The distribution moves in time with roughly constant width until centered on  $Q_{\text{eq}}$ . We have made a

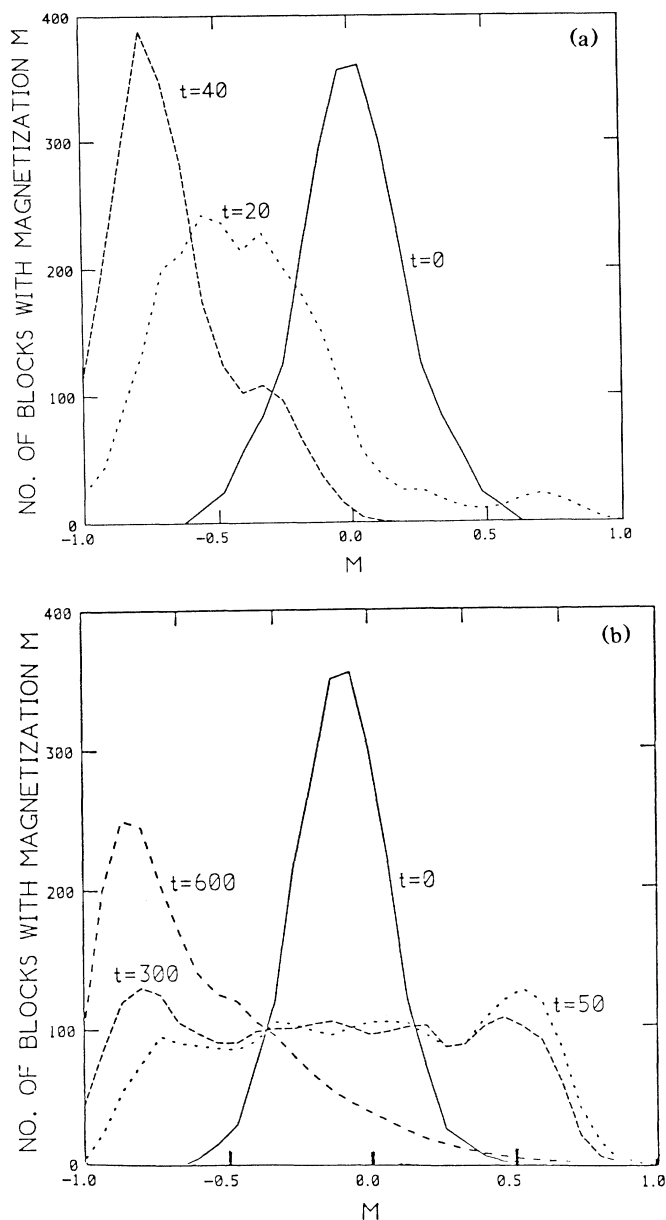


FIG. 3. Profiles of the number of  $3 \times 3 \times 3$  sub-blocks with a certain magnetization in a  $15 \times 15 \times 15$  simple cubic system which is quenched from far above  $T_c$  to around  $0.9T_c$ . Different profiles are for different times after the quench with one time unit corresponding to one flip attempt per spin. (a) Spin-strain coupling of the type  $XY + XZ + YZ$  only. (b) Direct nearest-neighbor spin-spin coupling only.

detailed study of the dynamics, to be published elsewhere,<sup>17,18</sup> in relation to the rate law discussed by Salje.<sup>19</sup> In general terms the stain-coupled system follows MFT behavior because the system remains effectively uniform. Figure 3(b) shows the contrasting case of a conventional nearest-neighbor Ising model (no strain coupling) adjusted to have the same  $T_c$ . We see

that at time  $t = 50$  the system has evolved to a broad distribution showing clusters with  $Q = \pm Q_{eq}$ , the boundaries between clusters accounting for the distribution in between these values. Then, after a very much longer time, the clusters with negative  $Q$  grow at the expense of those with positive  $Q$  to give the ordered state, not yet fully achieved at  $t = 600$ .

---

<sup>1</sup>E. Salje, B. Kuschoeche, B. Wruck, and H. Kroll, Phys. Chem. Min. **12**, 99 (1985).

<sup>2</sup>E. Salje, *Phase Transitions in Ferroelastic and Co-elastic Crystals* (Cambridge Univ. Press, Cambridge, 1990).

<sup>3</sup>E. Salje, B. Wruck, and H. Thomas (to be published).

<sup>4</sup>S. Marais and V. Heine (to be published).

<sup>5</sup>J. D. Eshelby, Solid State Phys. **3**, 97 (1956).

<sup>6</sup>E. Salje, Phys. Chem. Min. **14**, 455 (1987).

<sup>7</sup>S. A. T. Redfern *et al.*, J. Phys. C **21**, 277 (1988).

<sup>8</sup>J. W. Cahn and G. E. Hilliard, J. Chem. Phys. **28**, 258 (1958).

<sup>9</sup>H. Furukama, Adv. Phys. **34**, 703 (1985).

<sup>10</sup>J. S. Langer, M. Bar-on, and H. D. Miller, Phys. Rev. A **11**, 1417 (1975).

<sup>11</sup>S. Marais, V. Heine, and E. Salje (to be published).

<sup>12</sup>E. Salje, Ferroelastics **104**, 111 (1990).

<sup>13</sup>R. J. Glauber, J. Math. Phys. **4**, 294 (1963).

<sup>14</sup>J. Sapriel, Phys. Rev. B **12**, 5128 (1975).

<sup>15</sup>S. Marais and V. Heine (to be published).

<sup>16</sup>K. Binder, *Monte Carlo Methods in Statistical Physics* (Springer-Verlag, Berlin, 1986), p. 195.

<sup>17</sup>S. Marais, E. Salje, and V. Heine (to be published).

<sup>18</sup>S. Dattagupta, V. Heine, S. Marais, and E. Salje (to be published).

<sup>19</sup>E. Salje, Phys. Chem. Min. **15**, 336 (1988).